HHS Public Access

Author manuscript

J Comp Neurol. Author manuscript; available in PMC 2019 August 15.

Published in final edited form as:

J Comp Neurol. 2018 August 15; 526(12): 1978–1990. doi:10.1002/cne.24468.

Sensitivity and Specificity of Phospho-Ser129 α-Synuclein Monoclonal Antibodies

Vedad Delic, **Sidhanth Chandra**, **Hisham Abdelmotilib**, **Tyler Maltbie**, **Shijie Wang**, **Danielle Kem**, **Hunter J. Scott**, **Rachel N. Underwood**, **Zhiyong Liu**, **Laura A. Volpicelli-Daley**, and **Andrew B. West***

Center for Neurodegeneration and Experimental Therapeutics, Department of Neurology, University of Alabama at Birmingham, Birmingham, AL 35233 USA

Abstract

α-Synuclein (α-syn) is an abundant presynaptic protein that is the primary constituent of inclusions that define Lewy body diseases (LBDs). In these inclusions, α-syn is phosphorylated at the serine-129 residue. Antibodies directed to this phosphorylation site are used to measure inclusion abundance and stage disease progression in pre-clinical models as well as in post-mortem tissues in LBDs. While it is critical to reliably identify inclusions, phospho-specific antibodies often cross-react with non-specific antigens. Four commercially available monoclonal antibodies, two from rabbits (clones EP1536Y and MJF-R13) and two from mice (81a and pSyn#64), have been the most widely used in detecting pS129-α-syn inclusions. Here, we systematically evaluated these antibodies in brain sections and protein lysates from rats and mice. All antibodies detected pS129-α-syn inclusions in the brain that were induced by preformed α-syn fibrils in wild-type rats and mice. Antibody titrations revealed that clones EP1536Y and 81a comparably labeled inclusions in both the perikarya and neuronal processes in contrast to clones MJF-R13 and pSyn#64 that incompletely labeled inclusions at various antibody concentrations. Except for EP1536Y, the clones produced non-specific diffuse neuropil labeling in α-syn knockout mice as well as mice and rats injected with monomeric α-syn, with some non-specific staining titrating with pS129-α-syn inclusions. By immunoblot, all the clones cross-reacted with proteins other than α-syn, warranting caution in interpretations of specificity. Clone EP1536Y uniquely and robustly detected endogenous pS129-α-syn in highly soluble protein fractions from the mouse brain. In summary, EP1536Y had the highest sensitivity and specificity for detecting pS129-α-syn.

Graphical abstract

*Corresponding Author information: abwest@uab.edu Ph: 205 996 7697, Address: 1719 6th Ave. S., Birmingham, AL 35294.

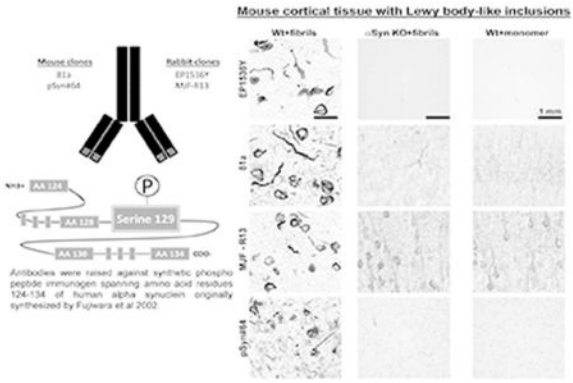

All antibodies detected pS129-α-syn inclusions in the brain induced by pre-formed α-syn fibrils in wild-type mice. Except for EP1536Y, the clones directed to phospho serine 129 residue of alpha synuclein (α-syn) produced non-specific diffuse neuropil labeling in α-syn knockout mice as well as mice injected with monomeric α-syn.

Keywords

SNCA; Lewy bodies; Lewy neurites; NACP; RRID P20 NS092530; RRID R01 NS064934; RRID R33 NS09764

INTRODUCTION

Lewy body and Lewy neurite inclusions consist predominantly of hyper-phosphorylated (Fujiwara et al., 2002) and insoluble α-synuclein (α-syn), hallmarks of Parkinson's disease (PD) and other Lewy body diseases (LBDs). α-Syn is encoded by the *SNCA* gene located on chromosome 4q21-q23 and is genetically linked to PD and Dementia with Lewy Bodies susceptibility (Chen et al., 1995; Polymeropoulos et al., 1996).

α-Syn is an abundant protein in neurons with a minimal fraction phosphorylated at serine 129. In contrast, in PD and LBD brains, >90% of α-syn in inclusions may be phosphorylated (Oueslati, 2016). Because phosphorylation at serine 129 distinguishes normal α-syn from abnormal α-syn, particularly α-syn in proteinaceous inclusions, numerous antibodies have been developed to peptides spanning the pS129 residue that is identical in humans and rodents. Four commercially available monoclonal antibodies to pS129-α-syn are available including: mouse clone 81a (IgG2a), EP1536Y (rabbit IgG), MJF-R13 (rabbit IgG), and pSyn#64 (mouse IgG1).

pS129-α-syn inclusion abundance significantly but imperfectly correlates with neurodegeneration and clinical phenotypes in LBDs (Gomez-Tortosa et al., 2000; Burke et al., 2008; Halliday et al., 2008). The accurate detection and estimation of α-syn inclusion abundance is fundamental to many pre-clinical and pathology studies. Herein, we performed systematic studies utilizing wild-type mice and rats harboring pS129-α-syn inclusions induced by the injection of short mouse α-syn fibrils together with α-syn knockout mice as controls. Short mouse α-syn fibrils are generated by aggregating monomeric α-syn into

higher order pre formed fibrils which are then fragmented by sonication into short fibrils (Polinski et al., 2018). Once injected into the murine brains the short α-syn fibrils are internalized in neurons where they serve as a template for new fibers. Fibrilization results in hyper phosphorylation of serine 129-α-syn similar to LBs. Some evidence suggests that LBs may be hyper phosphorylated through the action of polo-like kinases (Waxman and Giasson, 2011). Therefore, pS129-α-syn provides a reliable epitope for the detection of pathological inclusions distinct from non-fibrillized α-syn present at high concentrations in many neurons.

Herein, we utilize a panel of tissue procured from mice and rats exposed to short α-syn fibrils, together with α-syn knockout mouse controls, to define the specificity and sensitivity of commercially available monoclonal antibodies. Through these studies, we provide recommendations for more reliable detection of pS129-α-syn inclusions in model systems.

RESULTS

Reliability of α-syn inclusion detection in mouse and rat brain tissue using pS129-α-syn monoclonal antibodies

We and others have previously reported that injection with mouse derived pre-formed α-syn fibrils into the dorsal striatum of mice and rats causes profound α-syn inclusion pathology throughout the cortex and striatum (Luk et al., 2012; Masuda-Suzukake et al., 2014; Paumier et al., 2015; Abdelmotilib et al., 2017; Shimozawa et al., 2017). In contrast, α-syn knockout mice, or mice injected with only monomeric α-syn, do not develop these inclusions or pathology (Luk et al., 2012; Masuda-Suzukake et al., 2014; Abdelmotilib et al., 2017). α-Syn inclusions can be distinguished from endogenous α-syn due to phosphorylation (compared to α-syn not in inclusions) at the α-syn S129 residue. To compare four commercially available pS129-α-syn antibodies (Table 1) in brain sections from mice and rats, we used the antibodies at three concentrations (1, 10, and 100 ng mL^{-1}) with methods previously used for the antibody clone 81a in mouse tissue (Abdelmotilib et al., 2017). All antibodies robustly labeled inclusions in both the cortex and striatum at the 10 ng mL^{-1} concentration (Figure 1). Severe signal loss occurred for all antibodies at 1 ng mL^{-1} and no differences in signal for inclusions was observed between 10 and 100 ng mL^{-1} in either mouse or rat brains (Figure 5). In serial sections from the same mice, clones 81a and EP1536Y produced similar inclusion staining patterns. Prominent serpentine inclusions of significantly length were labeled with equal intensities as somal skein-like, often perinuclear, inclusions that could occupy much of the cytoplasm. In contrast, MJF-R13 and pSyn#64 showed more punctate perinuclear staining, with much weaker profiles of serpentine inclusions in the same affected tissue, particularly in neuron processes.

In cortical and striatal sections from α-syn knockout mice, or in wild-type mice injected with monomeric protein, clone EP1536Y did not produce appreciable signal (Figure 1a). However, clone 81a, in both sections from α-syn knockout mice and monomer injected wild type mice, produced diffuse neuropil staining in the cortex, particularly the somato-dendritic regions of pyramidal neurons (Figure 1b5, 1b7, 1b9, 1b11). Occasional cell processes reminiscent of endothelia were also labeled by 81a (Figure 1b7). However, this pattern of staining was not prominent in sections from fibril-injected mice and abundant pS129-α-syn

inclusions. These results suggest that in the absence of a specific epitope, at 10 ng mL^{-1}, the 81a antibody binds more non-specifically presumably to lower-affinity epitopes. In the striatum, clone 81a labeled axon bundles known as Wilson's pencils, both in control and in fibril injected sections (Figure 1b10, 1b12). Clone MJF-R13 also produced non-specific staining different than 81a in the cortex and striatum in α-syn knockout sections or wild-type mice injected with monomeric α-syn. Non-specific staining from clone pSyn#64 was minimal and consisted of non-descript lightly colored spots visible only at high-magnification (Figure 1d7,8), different from secondary-only antibody treated sections (Figure 2). Like pSyn#64, clone EP1536Y produced acceptable specificity, even in the absence of any inclusions in the sections. These results indicate EP1536Y and pSyn#64 as having higher specificity compared to clones 81a and MJF-R13.

Rats and mice share the same amino-acid sequence surrounding the pS129 residue in α-syn protein. In coronal frozen brain sections from rats, the same patterns of inclusion morphology were detected with each antibody, and similar off-target staining profiles were also observed (Figure 3). Subtle differences between the rat sections versus the sections from mice include morphological differences in labeled inclusion structures between antibodies EP1536Y and pSyn#64. EP1536Y labeling many more inclusions in neuronal processes both in the cortex and striatum compared to pSyn#64 (Figure 3a3,4, and Figure 3d3,4). The preference in MJF-R13 labeling cytoplasmic inclusions compared to inclusions in neuronal processes also appeared exaggerated in rats compared to the same trend in mice (Figure 3 c7,11). Overall, similar conclusions can be drawn for the performance of the antibody clones in rats and mice.

α-Syn monoclonal antibodies intensely label intracellular bodies in the α-syn knockout brain

In α-syn models as well as in human post-mortem tissue, α-syn inclusions are not always abundant and can be rare, yet the presence of rare inclusions can be profoundly important for interpretation. Because of the amount of staining we observed in the α-syn knockout mouse that cannot be accounted for by species-antibody (secondary) detection problems (Figure 2), we wondered whether there were sparse off-target staining features that could potentially be confused with pS129-α-syn inclusions. Serial sections across the whole α-syn knockout mouse brain were evaluated. Outside of the weaker off-target neuronal process staining associated with antibody clone 81a, more intense but rare small deposits of signal could be observed sparsely but uniformly through the somatosensory cortex (Figure 4a). In contrast, in brains that lacked pS129-α-syn inclusions, these structures could not be detected (Figure 1). The off-target signals in the knockouts highlighted different intracellular deposits with morphology different from the nearby motor cortex, although with similar intensity, and were typically smaller than pS129-α-syn inclusions. In both the somatosensory and motor cortex, clone MJF-R13 developed punctate intracellular staining profiles throughout the neuronal perikarya in many neurons (Figure 4b). MJF-R13 also labeled sparse intracellular puncta in both the insular cortex and nucleus accumbens. While pSyn#64 demonstrated exceptional overall specificity, occasional staining was observed under high-magnification analysis in very small (e.g., less than 5 microns) intracellular deposits in the motor, somatosensory, and insular cortices. Thus, we find that in the absence of the pS129-α-syn

antigen, clones MJF-R13, pSyn#64 and 81a non-specifically labeled different intracellular features in cells, some common and some rare, all with different morphologies. In contrast, antibody clone EP1536Y did not develop any significant labeled features in the α-syn knockout brain, even at higher concentrations in wild-type mouse brain that lacked inclusions. Therefore, EP1536Y shows the highest specificity for immunohistochemistry of pS129-α-syn inclusions, as well as comparable sensitivity to clone 81a.

Off-target pS129-α-syn staining titrates with the staining of α-syn inclusions

We next determined whether it was possible to further titrate the pS129-α-syn antibody so that inclusions and not the off-targets we described could be labeled However, in lowering the concentration of antibody to 1 ng mL^{-1}, pS129-α-syn α-syn inclusions were poorly labeled and difficult to image, even with the two antibodies that most intensely labeled inclusions (clones 81a and EP1536Y, Figure 5a1, b1). Increasing the concentration to 100 ng mL^{-1} did not improve the labeling of inclusions but greatly increased off-target and non-specific staining profiles (Figure 5a,c,e,g,a and Figure 5d,f,h,d). Similar results with clones MJF-R13 and pSyn#64 were obtained, with off-target staining increasing at the 100 ng mL^{-1} concentration. These results show it is not possible, using the staining conditions and blocking agents described here, to titrate off-target and non-specific signals from the labeling of pS129-α-syn inclusions.

pS129-α-syn monoclonal antibodies highlight different inclusion morphologies

Immunohistochemistry results with typical widefield microscopy show that the monoclonal antibodies differentially labeled the inclusions. To further investigate these differences in inclusion density and morphometry, we next obtained confocal images with optimal pinhole settings for a 63× objective with a numerical aperture of 1.4. Evaluation of single Z-planes through the inclusions revealed that clones 81a and EP1536Y labeling in a continuous swirl pattern that extended to the top and bottom borders of the neuron. As in widefield analysis, when stacked together these perinuclear structures presented as less-complex spheroids with decreased core density (Figure 6a,b). In contrast, pSyn#64 always labeled intense puncta along the skeins, with few or no instances of convincing serpentine structures in processes. These results suggest pSyn#64 does not continuously label across the fibrils and therefore explains the different morphologies observed in widefield microscopy.

Detection of off-target protein interactions with pS129-α-syn monoclonal antibodies using immunoblots

In addition to immunofluorescence and histochemistry approaches, pS129-α-syn is routinely quantified by immunoblotting lysates sequentially extracted into soluble and insoluble fractions from frozen brain tissue. Post-translational modifications can alter protein-protein interactions, solubility, and subcellular localization, which necessitates different tissue lysate preparations (e.g. high salt, detergent, and denaturants). We solubilized wild-type and α-syn knockout mouse brain tissue (non-perfused) into four sequential (serial-processed, w/v) solubilized fractions: 1) saline-only Dounce homogenization, 2) supplementation of high-salt (0.5M) with further Dounce homogenization, 3) supplementation with triton X-100 and sonication, and 4) supplementation with SDS and further sonication. A widely used and highly-specific monoclonal antibody directed to total α-syn, Syn1, demonstrated that most

α-syn protein (~18 kDa) could be detected in the triton X-100 extracted fraction in our protocol (Figure 7). As expected, in using anti-mouse secondary antibody with mouse brain lysate from non-perfused animals, weak heavy and light-chain signals for immunoglobulin were also detected in using mouse monoclonals 81a and pSyn#64. Antibody EP1536Y robustly detected a band near the expected size of non-phosphorylated α-syn in the most soluble fraction, just under the 20 kDa marker (~19 kDa), and this band was absent in the α-syn knockout lysates. Most of the endogenous pS129-α-syn was present in the saline-extracted fraction and did not need detergent for solubilization like total α-syn protein. pS129-α-syn could also be detected by EP1536Y in the triton-solubilized fraction, although it cannot be excluded that EP1536Y partially cross-reacts with non-phospho α-syn. These results show that endogenous pS129-α-syn is highly soluble and therefore subject to loss in standard tissue staining approaches that involve permeabilization of tissue and detergents.

Off-target binding of proteins other than α-syn was noted for all antibodies except for the Syn1 monoclonal to α-syn. Clone 81a detected a very robust band ~78 kD present exclusively in the SDS-extracted brain fraction whereas MJF-R13 detected an unknown protein of ~120 kDa exclusively in the saline-solubilized fraction. On longer exposures, MJF-R13 developed a high-molecular weight smear of protein labeling (e.g., >150 kDa extending to the top of the gel) that was comparable in both the α-syn knockout as well as wild-type mouse brain lysate. Clone EP1536Y also detected an off-target protein equally present in the soluble and triton-extracted fraction, similar to α-syn, of ~105 kDa in size. pSyn#64 cross-reacted only weakly with higher-molecular weight bands (~160 kDa), but the signal from the secondary-alone antibody was stronger than these off-target interactions. In summary, these results show that all of the pS129-α-syn monoclonal antibodies cross-react with proteins unrelated to α-syn and/or fail to detect pS129-α-syn protein in immunoblots from wild-type mouse brain lysates.

DISCUSSION

In this study, we compared commercially available monoclonal antibodies directed to the pS129-α-syn residue in the reliability and sensitivity of α-syn inclusion detection in rats and mice. Notably, different methods of preparing the tissue such as different antigen retrieval methods and blocking agents may affect antibody performance. Under the common conditions applied to all antibodies, inclusions were uniformly robustly detected at concentrations of 10 ng mL^{-1} and higher in both mice and rat brains while significant loss of signal was detected at 1 ng mL^{-1}. Clones 81a and EP1536Y detected similar inclusion profiles and densities in serial sections, whereas inclusions revealed by pSyn#64 and MJF-R13 were more limited and punctate in appearance. Problematic off-target staining, revealed in the α-syn knockout but also in wildtype mice and rats, titrated together with the labeling of inclusions in rodents exposed previously to α-syn fibrils. Some of these off-target proteins may have been detected by immunoblot, with all antibodies cross-reacting with different proteins that differ in size and solubility from that of α-syn.

Clone EP1536Y was the only antibody able to detect endogenous pS129-α-syn via immunoblot, and pS129-α-syn was much more soluble than total α-syn. As very little total α-syn was detected in the saline-only soluble fraction, these results are consistent with

pS129-α-syn constituting a small fraction of total α-syn. As all antibodies were raised against close variations of the same peptide, it is reasonable to conclude that EP1536Y has a higher affinity than the other antibodies towards the peptide conformation of the pS129-α-syn epitope as present on membranes in immunoblots. Some studies have reported improved success of α-syn peptide detection on immunoblots by changing the peptide conformations via fixation with paraformaldehyde or other cross-linking fixatives (Lee and Kamitani, 2011). It is possible that with additional protocol refinement, e.g. higher pH antigen retrieval buffer compared to pH 6.0 retrieval buffer used herein, the other monoclonal antibodies may be adapted to detect pS129-α-syn with better sensitivity than that reported here.

Here, we focused on rodent models because we could utilize knockout mice as definitive controls as well as rats treated with fibrils to induce robust pS129-α-syn positive inclusions in a controlled way. Rats also provide an additional source of brain tissue different than the species used to generate the antibody to avoid the potential problem of cross-reactive immunoglobulins. Rutherford et al recently presented a strong case that off-target interactions inherent to the antibody clone 81a has led to an overestimation of inclusion burden in several studies (Rutherford et al., 2016). In high-magnification imaging, we can confirm that clone 81a cross-reactivity is high, but is also unambiguously distinct from pS129-α-syn inclusions formed in neurons from exposure to fibrils. The other antibody clones did not share the off-target profiles of clone 81a. The biggest difference in pS129-α-syn inclusions from off-target intracellular staining is the small size of features associated with off-target staining in the cytosol, as well as the lack of filaments in neuronal processes and lack of clear skein structures in the perikarya.

In many studies, the small molecule thioflavin is used to confirm the presence of β-sheets that typify authentic amyloid. However, thioflavin has relatively weak affinity to most protein fibrils in cells that are typically in the mid-micromolar range (Ye et al., 2008; Sulatskaya et al., 2011; Lindberg et al., 2015) compared to all the monoclonal antibodies used here that show affinities in the low nanomolar to femptomolar range. Curiously, thioflavin-T and related molecules show high-affinity binding to α-syn fibrils *in vitro* but much lower to negligible affinity to inclusions in neurons (Ye et al., 2008). Thus, as a low-affinity binding molecule, titrations of thioflavin can easily produce false signal and should therefore be avoided as a confirmatory stain. Based on our results here, a better approach would be to apply several of the different monoclonal antibodies (e.g., a mouse and a rabbit monoclonal) in parallel because each antibody shows different off-target specificity but still very high affinity towards pS129-α-syn inclusions. Facilitating a co-labeling approach with conventional staining approaches, two of the monoclonals are rabbit Ig and two are mouse Ig. We further conclude that the α-syn knockout is an invaluable control since all of the antibodies appear to have the potential to interact with proteins other than α-syn.

In brain sections with clear α-syn inclusions and pathology, such as in the pre-formed fibril models of disease, calculations of inclusion pathologies based on intensity of signal may not be able to separate background from pS129-α-syn inclusions. Theoretically, matched sections from control animals could be used in subtractive approaches to account for off-target and nonspecific signals. Since wild-type animals showed the same staining pattern as α-syn knockout animals, it could be argued that α-syn knockout animals may not be

required for approaches where signal from control animals can be subtracted. However, the success of using wild-type and/or α-syn knockout animals as a background control depends on the labeled off-target proteins being stable in expression in disease states, and this is probably not the case for at least one suspected off target, phosphorylated neurofilament light-chain (Rutherford et al., 2016). Thus, high-magnification approaches that consider morphometries of inclusions may be the best way to quantify inclusion abundance. Further complicating interpretation is that brain sections filled with many inclusions may render antibodies less-available to off-target interactions, thereby compressing a signal (inclusions) to noise (off-targets) ratio.

Although all antibodies were raised to the same phosphorylated site in α-syn, the antibodies unexpectedly differed in their ability to fully label inclusions. EP1536Y and 81a produced fuller and more connected skeins through the neuronal cytoplasm as well as in processes, compared to pSyn#64 and MJF-R13. Due to the probable interaction of 81a with neurofilaments that titrate together with pS129-α-syn in inclusions (Rutherford et al., 2016), we therefore can conclude that EP1536Y is the antibody with the highest specificity and sensitivity of those tested. Warranting caution, EP1536Y detects an off-target higher-molecular weight protein unrelated to α-syn, but this protein was apparently not detected via immunohistochemistry or confocal approaches. Other tissue-chemistry protocols that might potentially unmask the cross-reactive EP1536Y epitope as seen in immunoblots could potentially confound interpretation with this antibody.

Outside of α-syn inclusions, we confirm the existence of endogenous pS129-α-syn only through immunoblots with EP1536Y. Unexpectedly, most of the endogenous pS129-α-syn protein appeared in a highly soluble protein fraction, released with only gentle Dounce homogenization in saline. Since this is the fraction of protein most difficult to retain in tissue-staining protocols, washed away with even small amounts of detergents, the innate biology of pS129-α-syn may also explain why it is incredibly difficult to localize within brain tissue. Unequivocally, phosphatases that normally remove phosphate from S129 lose their ability to interact when α-syn refolds into fibrils in cells. It is tempting to speculate that the more soluble and non-membrane bound α-syn subunits, like pS129-α-syn, are those more likely to participate in the formation of inclusions (Lue et al., 2012; Walker et al., 2013). Unfortunately, most observations regarding the biology of pS129-α-syn have been made using phospho-mimetic and phospho-null mutations in the S129 residue that may not preserve the temporal aspects of pS129-α-syn as well as the unique solubility profile. With the comparative analysis of the available monoclonal antibodies presented here, we hope that these observations and recommendations enable more definitive conclusions from both past and future studies that unravel the biology of α-syn in disease.

CONCLUSIONS

Antibody EP1536Y demonstrates the best reliability and pS129- α-syn inclusion detection sensitivities in mouse and rat brain, although usage of several antibodies in parallel is recommended to ensure reliability of results. Given the off-target and non-specific patterns of staining with all the antibodies, we did not obtain evidence that endogenous pS129-α-syn outside of inclusions could be labeled in brain sections.

METHODS

Animals

All animal protocols and procedures were approved by the University of Alabama at Birmingham (UAB) Institutional Animal Care and Use Committee. Sprague Dawley outbred rats were obtained from Taconic Farms, and C57BL/6 J mice and α-syn knockout mice were obtained from Jackson Laboratories.

Antibody Characterization

Ser(P)-129 α-syn antibodies and the antibody raised to total alpha synuclein were commercially available and purchased from Abcam (EP1536Y,81a, MJF-R13), Wako USA (pSyn#64), and BD Bioscience (Syn1). Vendors report that the Ser(P)-129 α-syn monoclonal antibodies were raised against synthetic human α-synuclein peptide spanning 124–134 region with a phosphorylated Ser 129 residue. This peptide sequence was originally constructed by Fujiwara et al, and used in their seminal work that led to the discovery of extensive α-syn phosphorylation at Ser 129 reside in Lewy bodies (Fujiwara et al., 2002). Monoclonal antibodies developed against synthetic α-syn aa 124–134 (phospho 129) peptide were validated using other antibodies that label Lewy bodies in post-mortem brain sections (Baba et al., 1998; Fujiwara et al., 2002).

Clone EP1536Y is a monoclonal IgG antibody raised in rabbit and may be suitable for use in immunoblotting and immunohistochemistry (Perez-Revuelta et al., 2014; Prusiner et al., 2015; Tuttle et al., 2016; Arawaka et al., 2017). Clone 81a is mouse IgG2a also used in immunoblot and immunohistochemistry applications (Tuttle et al., 2016; Dieriks et al., 2017). MJF-R13 is a rabbit IgG monoclonal antibody used in immunoblotting experiments (Brahmachari et al., 2016). Clone pSyn#64 is mouse IgG1 suitable for immunoblotting and immunohistochemistry (Jiang et al., 2016). Clone Syn1 is mouse IgG1 raised to rat α-syn peptide aa 15–123, has not been further mapped within that peptide, but has been previously evaluated for specificity (Perrin et al., 2003). For additional primary antibody information and secondary antibody information see Table 1. Optimal secondary concentration was determined by serial dilution starting with the vendor recommendations. pS129-α-syn antibody concentration was confirmed using a BCA Protein Assay Kit (Pierce) with a γ-globulin protein standard, and all antibodies diluted to working stock concentrations of 0.1 mg mL^{-1}.

Injections and tissue processing

8 to 10 week mice and rats were anesthetized using isoflurane and bilaterally injected into the dorsal striatum with sonicated α-syn fibrils, α-syn monomer, or saline as described (Abdelmotilib et al., 2017). Mice or rats were injected with 2 or 4 μl of solution respectively using a 32-gauge needle and Hamilton syringe over the course of 20 minutes. Solutions were injected in mice (and rats) in the right and left dorsal striatum at coordinates: 1.0 (0.7 rat) mm anterior and 1.85 (3.0 rat) mm lateral to the Bregma, and 3.0 (5.5 rat) mm ventral relative to the skull.

Animals were anesthetized 6 months post injection with isoflurane and transcardially perfused with room temperature phosphate buffered saline solution (PBS, pH 7.4) and then 4% paraformaldehyde (PFA) in PBS. The 6 month time point was experimentally determined to have severe and wide-spread inclusion burden throughout much of the basal ganglia (Abdelmotilib et al., 2017). Brains were removed and post-fixed in 4% PFA in PBS at 4°C for 24 hours with agitation, and then soaked in a 30% sucrose/PBS for 24 hours at 4°C. The brains were flash frozen in 2-methylbutane and later cut on a freezing sliding microtome into 40-micron sections.

Immunohistochemistry

For immunohistochemistry with 3,3'-diaminobenzidine (DAB), sections were quenched with 0.6% H_2O_2 in methanol for 45 minutes at room temperature (RT) with agitation. Following two 5 minute washes with tris buffered saline (TBS, pH 7.4), sections were incubated in antigen retrieval buffer (10mM Na Citrate, 0.05% Tween-20, pH 6.0) at 37°C for one hour at 40 rpm. Sections were washed with TBS 3 times for 5 minutes and then blocked with 5% horse (or 5% goat serum), TBS, and 3% triton x-100 (or 0.3% triton x-100) for 1 hour. Sections were washed 2× five minute with TBS, and primary antibodies detecting α-syn phosphorylated on Ser129 were added in blocking solution containing 1% horse (or 1% goat serum), TBS, 0.1% triton x-100 (or 0.3% triton x-100) for 48 hours at 4°C with agitation. After 2 rinses with TBS, secondary antibodies in blocking solution with 2.5% horse serum (or 2.5% goat serum), TBS, 0.1% triton x-100 (or 0.3% triton x-100) were added for 4 hours at 4°C with agitation. Sections were washed and then incubated for 1 minute in ABC solution (Vector) for amplification of signal. Sections were then washed and developed using Impact DAB Chromogen Solution (Vector). Sections were mounted on slides after 2 washes with TBS and then progressively dehydrated using ethanol and Histo-clear, rehydrated with water, and then dehydrated with ethanol and Histo-clear again. Slides were coversliped using Permount®. Sections were Imaged using Olympus BX61 microscope.

For fluorescence, sections were washed twice with TBS and incubated in antigen retrieval buffer at 37°C for 30 minutes on shaker 30 RPM and then blocked in 5% goat serum, TBS, and 0.3% triton x-100 for 1 hr. After two washes, primary antibodies at 20 ng mL^{-1} added in a blocking solution (5% goat serum, TBS, and 0.1% triton x-100) for 24 hours at 4°C with agitation. Following three washes, the secondary antibodies (Alexa 488 conjugated goat anti rabbit or goat anti mouse) were added in a blocking solution (5% goat serum, TBS, and 0.1% triton x-100) for 24 hours at 4°C with agitation. Sections were mounted on slides, and coverslips were applied using ProLong gold. Confocal images were captured using a Leica TCS-SP5

Protein Lysate Preparation

Mice were perfused with 20 mL of ice cold PBS and the brains were removed. Brain tissue (150 mg) was placed in to 1 mL of TBS with 2× protease inhibitors and phosphatase inhibitors. Following 10 strokes of Dounce homogenization, samples were centrifuged for 10 minutes at 20,000 g at 4°C. 500 μl of supernatant was then combined with 500 μl of 2× laemmli buffer to create PBS fraction lysate. The pellet was resuspended in 1 mL of TBS

supplemented to 500 nM NaCl and 2× protease inhibitors and phosphatase inhibitors with 15 strokes of Dounce homogenization. The sample was then centrifuged for 10 minutes at 20,000 g at 4°C, and 500 μl of supernatant was combined with 500 μl of 2× Laemmli buffer to create high salt fraction lysate. The pellet was resuspended in 1 mL of TBS supplemented to 500 nM NaCl, 1% triton x-100, 2× protease inhibitors and phosphatase inhibitors by vortexing for 30 seconds and rotating on a wheel for an hour. The sample was then centrifuged for 10 minutes at 20,000 g at 4°C, and 500 μl of supernatant was combined with 500 μl of 2× Laemmli buffer to create Triton fraction lysate. The pellet was resuspended in 1 mL of TBS supplemented to 500 nM NaCl, 1% (w/v) SDS, 2× protease inhibitors and phosphatase inhibitors by sonicating for 20 seconds. The sample was then centrifuged for 10 minutes at 20,000 g at 4°C, and 500 μl of supernatant was combined with 500 μl of 2× Laemmli buffer to create the SDS lysate fraction.

Immunoblotting analysis

Samples were thawed on ice and boiled for 5 minutes at 90°C. After use of crescendo, 20 μl of protein was loaded into a 10 well 4–20% gel. The gel was run at 100 mV for 1 hour, and transferred to a nitrocellulose membrane overnight at 4°C. Following a rinse with TBS, nonspecific sites were blocked with 5% milk in TBST for 1 hour at RT. Primary antibodies were applied at 1:2500 concentration in 5% milk in TBST overnight at 4°C. Following three 5 minute washes with TBST, secondary antibodies were applied at a 1:10000 concentration in 5% milk in TBST overnight at 4°C. After 3 washes with TBST, the membrane was incubated with Crescendo for 1 minute. Membranes were digitally imaged on a ChemiDoc system.

Acknowledgments

This work was supported by NIH/NINDS grants R01 NS064934, P20 NS092530, and R33 NS09764. The authors are grateful to Valentina Krendelchtchikova for assistance with the production of recombinant α-syn, and Xianzhen “Jane” Hu for stereotaxic surgeries and rat colony maintenance. We would like to acknowledge Kaela Kelly, Nicole Bryant, and Victoria Huang for manuscript review.

References

Abdelmotilib H, Maltbie T, Delic V, Liu Z, Hu X, Fraser KB, Moehle MS, Stoyka L, Anabtawi N, Krendelchtchikova V, Volpicelli-Daley LA, West A. alpha-Synuclein fibril-induced inclusion spread in rats and mice correlates with dopaminergic Neurodegeneration. Neurobiol Dis. 2017; 105:84–98. [PubMed: 28576704]

Arawaka S, Sato H, Sasaki A, Koyama S, Kato T. Mechanisms underlying extensive Ser129-phosphorylation in alpha-synuclein aggregates. Acta Neuropathol Commun. 2017; 5(1):48. [PubMed: 28619113]

Baba M, Nakajo S, Tu PH, Tomita T, Nakaya K, Lee VM, Trojanowski JQ, Iwatsubo T. Aggregation of alpha-synuclein in Lewy bodies of sporadic Parkinson's disease and dementia with Lewy bodies. Am J Pathol. 1998; 152(4):879–884. [PubMed: 9546347]

Brahmachari S, Ge P, Lee SH, Kim D, Karuppagounder SS, Kumar M, Mao X, Shin JH, Lee Y, Pletnikova O, Troncoso JC, Dawson VL, Dawson TM, Ko HS. Activation of tyrosine kinase c-Abl contributes to alpha-synuclein-induced neurodegeneration. J Clin Invest. 2016; 126(8):2970–2988. [PubMed: 27348587]

Burke RE, Dauer WT, Vonsattel JP. A critical evaluation of the Braak staging scheme for Parkinson's disease. Ann Neurol. 2008; 64(5):485–491. [PubMed: 19067353]

Chen X, de Silva HA, Pettenati MJ, Rao PN, St George-Hyslop P, Roses AD, Xia Y, Horsburgh K, Ueda K, Saitoh T. The human NACP/alpha-synuclein gene: chromosome assignment to 4q21.3-q22 and TaqI RFLP analysis. Genomics. 1995; 26(2):425–427. [PubMed: 7601479]

Dieriks BV, Park TI, Fourie C, Faull RL, Dragunow M, Curtis MA. alpha-synuclein transfer through tunneling nanotubes occurs in SH-SY5Y cells and primary brain pericytes from Parkinson's disease patients. Sci Rep. 2017; 7:42984. [PubMed: 28230073]

Fujiwara H, Hasegawa M, Dohmae N, Kawashima A, Masliah E, Goldberg MS, Shen J, Takio K, Iwatsubo T. alpha-Synuclein is phosphorylated in synucleinopathy lesions. Nat Cell Biol. 2002; 4(2):160–164. [PubMed: 11813001]

Gomez-Tortosa E, Irizarry MC, Gomez-Isla T, Hyman BT. Clinical and neuropathological correlates of dementia with Lewy bodies. Ann N Y Acad Sci. 2000; 920:9–15. [PubMed: 11193181]

Halliday G, Hely M, Reid W, Morris J. The progression of pathology in longitudinally followed patients with Parkinson's disease. Acta Neuropathol. 2008; 115(4):409–415. [PubMed: 18231798]

Jiang P, Gan M, Yen SH, Moussaud S, McLean PJ, Dickson DW. Proaggregant nuclear factor(s) trigger rapid formation of alpha-synuclein aggregates in apoptotic neurons. Acta Neuropathol. 2016; 132(1):77–91. [PubMed: 26839082]

Lee BR, Kamitani T. Improved immunodetection of endogenous alpha-synuclein. PLoS One. 2011; 6(8):e23939. [PubMed: 21886844]

Lindberg DJ, Wranne MS, Gilbert Gatty M, Westerlund F, Esbjorner EK. Steady-state and time-resolved Thioflavin-T fluorescence can report on morphological differences in amyloid fibrils formed by Abeta(1–40) and Abeta(1–42). Biochem Biophys Res Commun. 2015; 458(2):418–423. [PubMed: 25660454]

Lue LF, Walker DG, Adler CH, Shill H, Tran H, Akiyama H, Sue LI, Caviness J, Sabbagh MN, Beach TG. Biochemical increase in phosphorylated alpha-synuclein precedes histopathology of Lewy-type synucleinopathies. Brain Pathol. 2012; 22(6):745–756. [PubMed: 22369130]

Luk KC, Kehm V, Carroll J, Zhang B, O'Brien P, Trojanowski JQ, Lee VM. Pathological alpha-synuclein transmission initiates Parkinson-like neurodegeneration in nontransgenic mice. Science. 2012; 338(6109):949–953. [PubMed: 23161999]

Masuda-Suzukake M, Nonaka T, Hosokawa M, Kubo M, Shimozawa A, Akiyama H, Hasegawa M. Pathological alpha-synuclein propagates through neural networks. Acta Neuropathol Commun. 2014; 2:88. [PubMed: 25095794]

Oueslati A. Implication of Alpha-Synuclein Phosphorylation at S129 in Synucleinopathies: What Have We Learned in the Last Decade? J Parkinsons Dis. 2016; 6(1):39–51. [PubMed: 27003784]

Paumier KL, Luk KC, Manfredsson FP, Kanaan NM, Lipton JW, Collier TJ, Steece-Collier K, Kemp CJ, Celano S, Schulz E, Sandoval IM, Fleming S, Dirr E, Polinski NK, Trojanowski JQ, Lee VM, Sortwell CE. Intrastriatal injection of pre-formed mouse alpha-synuclein fibrils into rats triggers alpha-synuclein pathology and bilateral nigrostriatal degeneration. Neurobiol Dis. 2015; 82:185–199. [PubMed: 26093169]

Perez-Revuelta BI, Hettich MM, Ciociaro A, Rotermund C, Kahle PJ, Krauss S, Di Monte DA. Metformin lowers Ser-129 phosphorylated alpha-synuclein levels via mTOR-dependent protein phosphatase 2A activation. Cell Death Dis. 2014; 5:e1209. [PubMed: 24810045]

Perrin RJ, Payton JE, Barnett DH, Wraight CL, Woods WS, Ye L, George JM. Epitope mapping and specificity of the anti-alpha-synuclein monoclonal antibody Syn-1 in mouse brain and cultured cell lines. Neurosci Lett. 2003; 349(2):133–135. [PubMed: 12946570]

Polinski NK, Volpicelli-Daley LA, Sortwell CE, Luk KC, Cremades N, Gottler LM, Froula J, Duffy MF, Lee VM, Martinez TN, Dave KD. Best Practices for Generating and Using Alpha-Synuclein Pre-Formed Fibrils to Model Parkinson's Disease in Rodents. J Parkinsons Dis. 2018

Polymeropoulos MH, Higgins JJ, Golbe LI, Johnson WG, Ide SE, Di Iorio G, Sanges G, Stenroos ES, Pho LT, Schaffer AA, Lazzarini AM, Nussbaum RL, Duvoisin RC. Mapping of a gene for Parkinson's disease to chromosome 4q21-q23. Science. 1996; 274(5290):1197–1199. [PubMed: 8895469]

Prusiner SB, Woerman AL, Mordes DA, Watts JC, Rampersaud R, Berry DB, Patel S, Oehler A, Lowe JK, Kravitz SN, Geschwind DH, Glidden DV, Halliday GM, Middleton LT, Gentleman SM, Grinberg LT, Giles K. Evidence for alpha-synuclein prions causing multiple system atrophy in

humans with parkinsonism. Proc Natl Acad Sci U S A. 2015; 112(38):E5308–5317. [PubMed: 26324905]

Rutherford NJ, Brooks M, Giasson BI. Novel antibodies to phosphorylated alpha-synuclein serine 129 and NFL serine 473 demonstrate the close molecular homology of these epitopes. Acta Neuropathol Commun. 2016; 4(1):80. [PubMed: 27503460]

Shimozawa A, Ono M, Takahara D, Tarutani A, Imura S, Masuda-Suzukake M, Higuchi M, Yanai K, Hisanaga SI, Hasegawa M. Propagation of pathological alpha-synuclein in marmoset brain. Acta Neuropathol Commun. 2017; 5(1):12. [PubMed: 28148299]

Sulatskaya AI, Kuznetsova IM, Turoverov KK. Interaction of thioflavin T with amyloid fibrils: stoichiometry and affinity of dye binding, absorption spectra of bound dye. J Phys Chem B. 2011; 115(39):11519–11524. [PubMed: 21863870]

Tuttle MD, Comellas G, Nieuwkoop AJ, Covell DJ, Berthold DA, Kloepper KD, Courtney JM, Kim JK, Barclay AM, Kendall A, Wan W, Stubbs G, Schwieters CD, Lee VM, George JM, Rienstra CM. Solid-state NMR structure of a pathogenic fibril of full-length human alpha-synuclein. Nat Struct Mol Biol. 2016; 23(5):409–415. [PubMed: 27018801]

Walker DG, Lue LF, Adler CH, Shill HA, Caviness JN, Sabbagh MN, Akiyama H, Serrano GE, Sue LI, Beach TG. Arizona Parkinson Disease C. Changes in properties of serine 129 phosphorylated alpha-synuclein with progression of Lewy-type histopathology in human brains. Exp Neurol. 2013; 240:190–204. [PubMed: 23201181]

Waxman EA, Giasson BI. Characterization of kinases involved in the phosphorylation of aggregated alpha-synuclein. J Neurosci Res. 2011; 89(2):231–247. [PubMed: 21162130]

Ye L, Velasco A, Fraser G, Beach TG, Sue L, Osredkar T, Libri V, Spillantini MG, Goedert M, Lockhart A. In vitro high affinity alpha-synuclein binding sites for the amyloid imaging agent PIB are not matched by binding to Lewy bodies in postmortem human brain. J Neurochem. 2008; 105(4):1428–1437. [PubMed: 18221373]

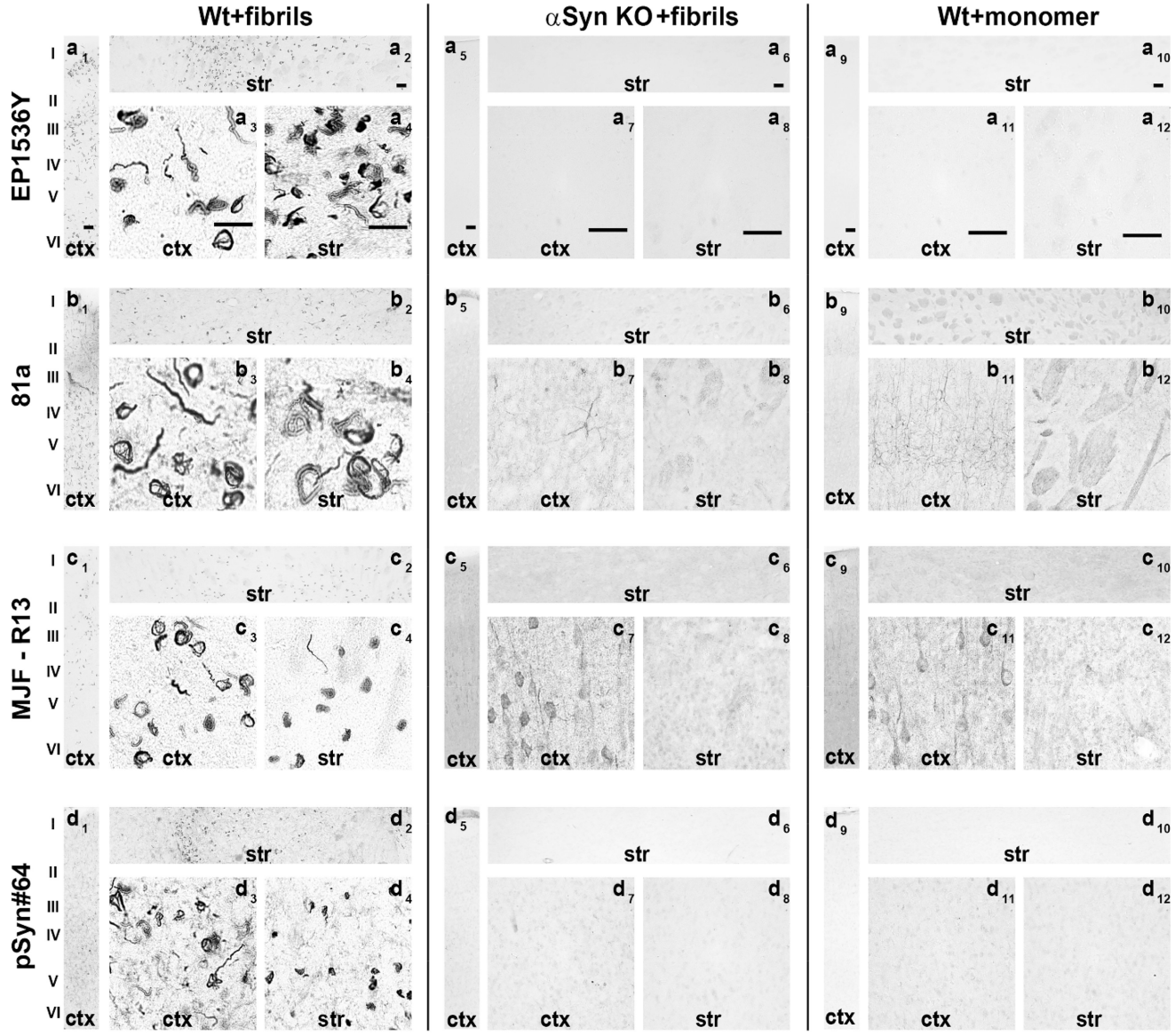

Fig. 1. Assessment of pSer129-α-Syn and inclusion detection in mouse brain

Wild-type and α-syn knockout mice (C57bl/6J) were injected bilaterally into the striatum with 10 μg of α-syn pre-formed fibrils or monomeric protein as previously described(Abdelmotilib et al., 2017). Brain sections were evaluated from mice six months later. Representative widefield images of DAB-staining (converted to grayscale for contrast) with the indicated monoclonal antibody (left margins) in animals injected with **A)** fibrils in wild-type mice, **B)** fibrils in α-Syn knockout mice, or **C)** monomer protein in wild-type mice. All antibodies were included at 10 ng mL^{-1} concentration. Coronal sections are shown with 0.4 mm of Bregma, with primary motor cortex (ctx) and dorsal striatum (str) shown at two different magnifications. Scale bars are 0.1 mm.

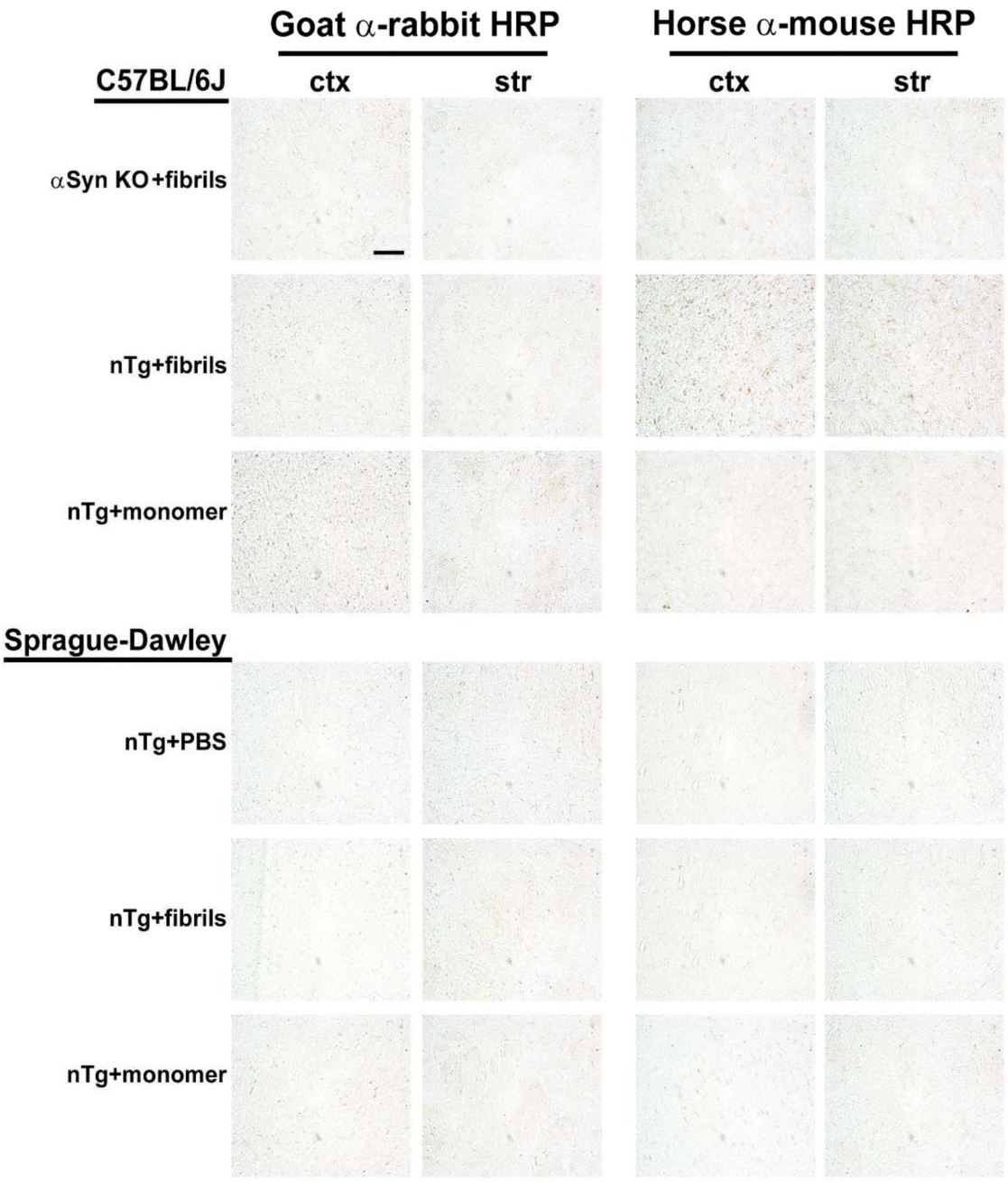

Fig. 2. Lack of signal in secondary-only (anti-mouse and anti-rabbit) antibody coronal brain sections

Wild-type and α-syn knockout mice (C57bl/6J) and wild-type Sprague Dawley rats (SDTac) were injected as indicated (left hand margins) bilaterally into the striatum, and processed six months later. Representative widefield images of DAB-staining (converted to grayscale for contrast) with the indicated secondary antibody (top margin). Coronal sections are shown near Bregma from primary motor cortex (ctx) and dorsal striatum (str), with the scale bar set to 0.1 mm.

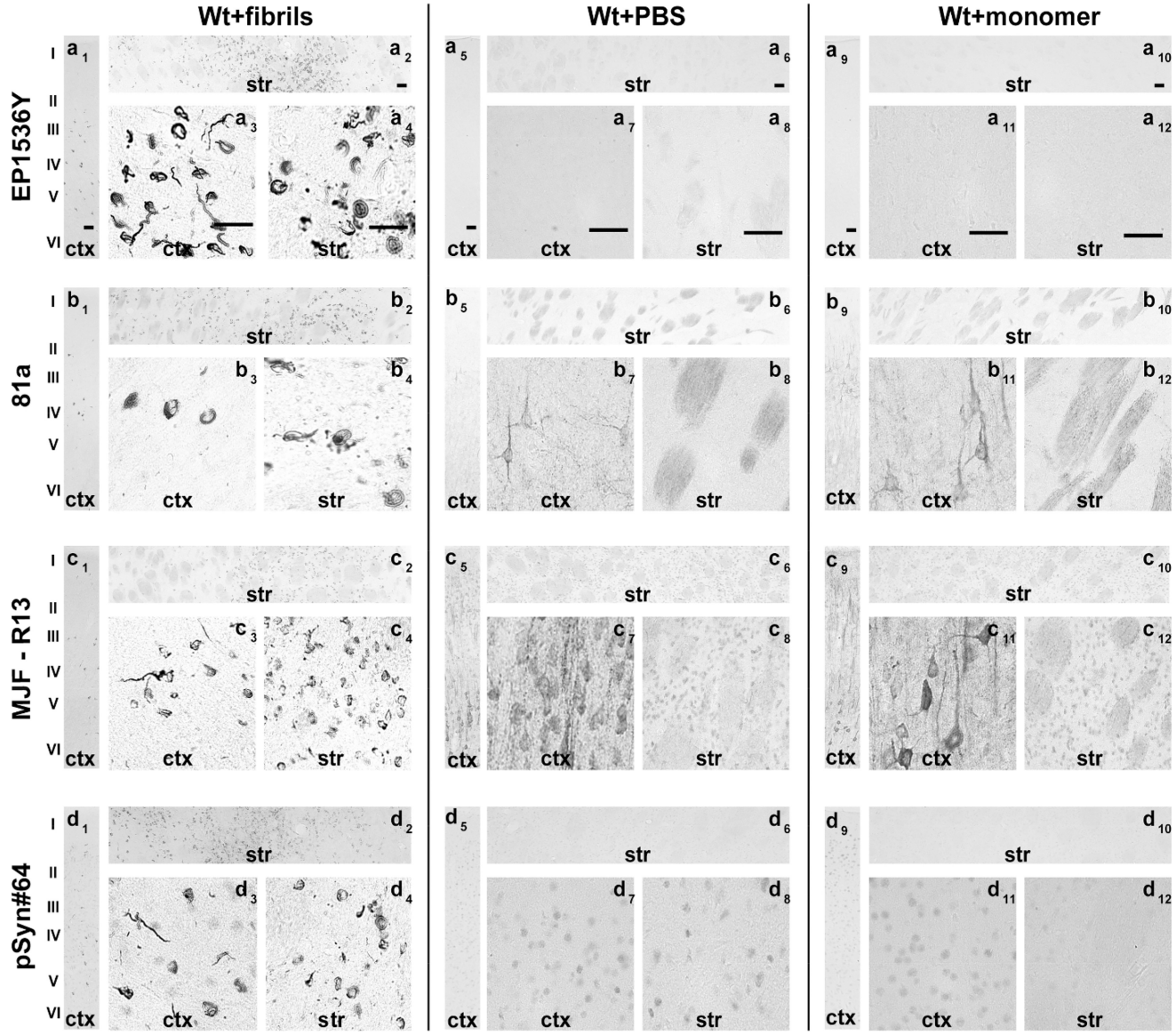

Fig. 3. Assessment of pSer129-α-Syn and inclusion detection in rat brain

Wild-type Sprague Dawley rats (SDTac) were injected bilaterally into the striatum with 20 μg of α-syn pre-formed fibrils or monomeric protein as previously described(Abdelmotilib et al., 2017). Brain sections were evaluated from rats six months later. Representative widefield images of DAB-staining (converted to grayscale for contrast) with the indicated monoclonal antibody (left margins) in animals injected with **A)** fibrils in wild-type rats, **B)** saline control in wild-type rats, and **C)** monomer protein in wild-type rats. All antibodies were included at 10 ng mL^{-1} concentration. Coronal sections are shown within ~1 mm of Bregma, with primary motor cortex (ctx) and dorsal striatum (str) shown at two different magnifications. Scale bars are 0.1 mm.

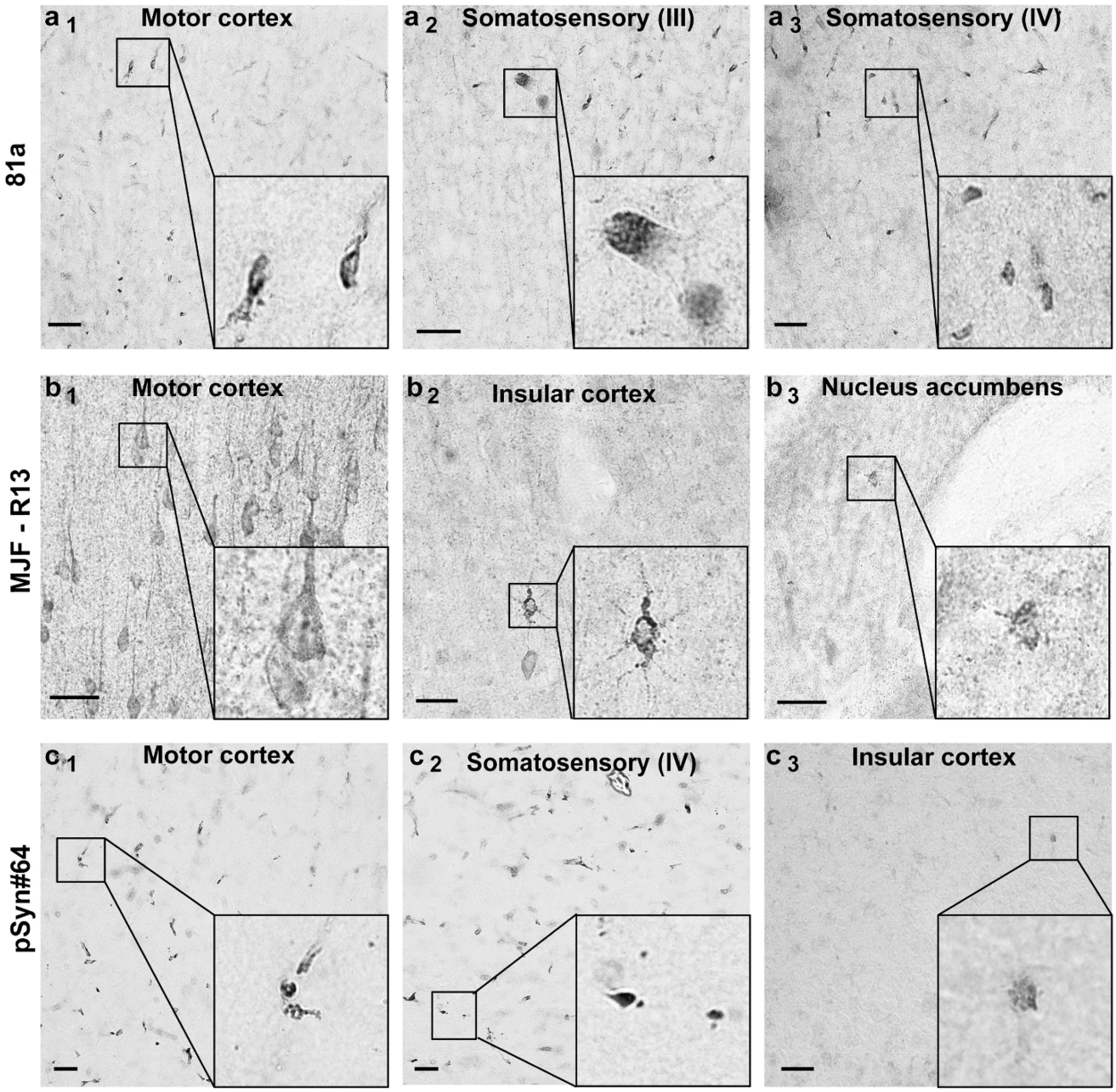

Fig. 4. Assessment of pSer129-α-syn monoclonal antibodies in α-syn knockout mice

Coronal brain sections were obtained from adult (3–6 months) α-syn knockout mice and evaluated with the monoclonal antibody indicated in the left margin (**a, b, c**), all used at 10 ng mL^{-1}. Representative images from DAB staining (grayscale shown for contrast) are shown. Insets black bounding boxes show higher magnifications of features of interest. Scale bars are 0.1 mm.

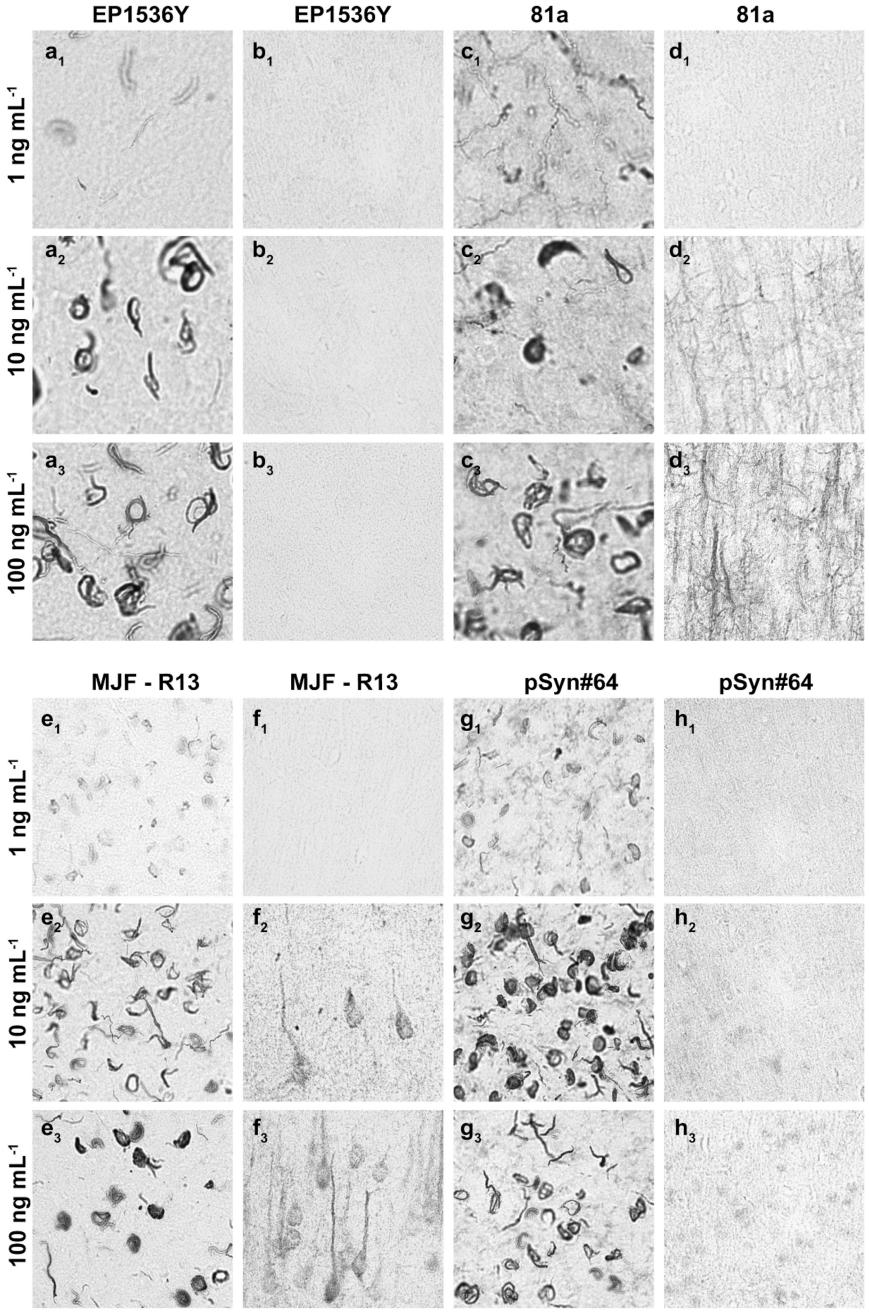

Fig 5. Off-target pSer129-α-syn monoclonal antibody staining titrates with the labeling of inclusions

Frozen coronal sections of primary motor cortex 0.4mm of Bregma from wild-type C57Bl/6J mice injected with α-syn fibrils in the striatum (a,b) or (**c,d,e,g**) non-injected wild-type mice were evaluated with the indicated monoclonal pSer129 α-syn antibody (top margin) at the indicated concentration (left margin).

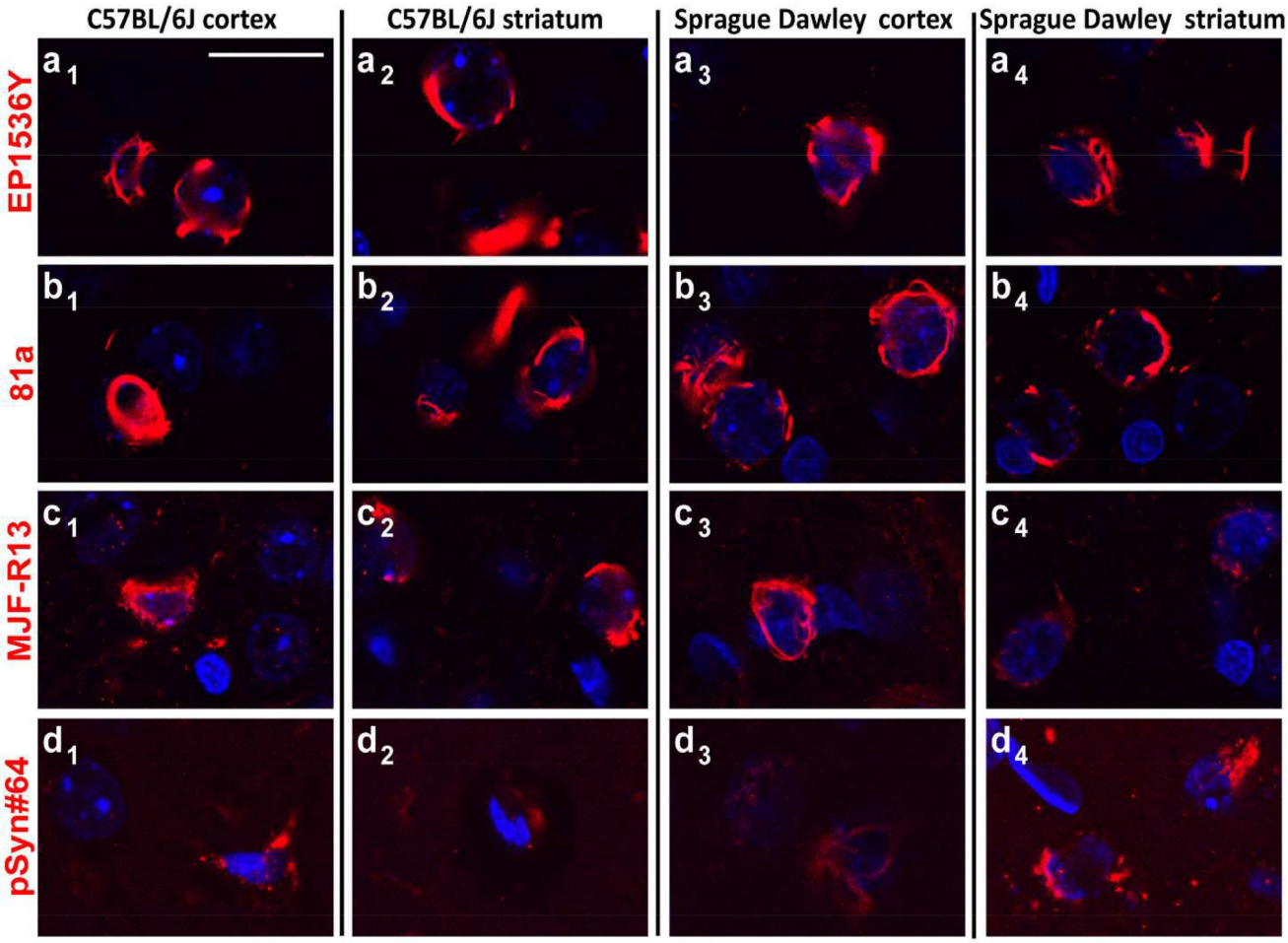

Fig 6. Confocal analysis of pS129 α-syn-positive inclusions in mice and rats

C57Bl/6J wild-type mice and Sprague Dawley wild-type rats were injected bilaterally into the striatum with either 10 μg or 20 μg (respectively) of α-syn fibrils and frozen brain sections analyzed six months later. Confocal images were obtained from a single plane with a 63× objective set for optimal pinhole. Red color indicates pS129-α-syn staining (Cy3) and blue color indicates DAPI. The monoclonal antibody used at 20 ng mL^{-1} are given in the left margin. Images from both the primary motor cortex (cortex) and dorsal striatum (striatum) were obtained. Scale bar is 50 μm.

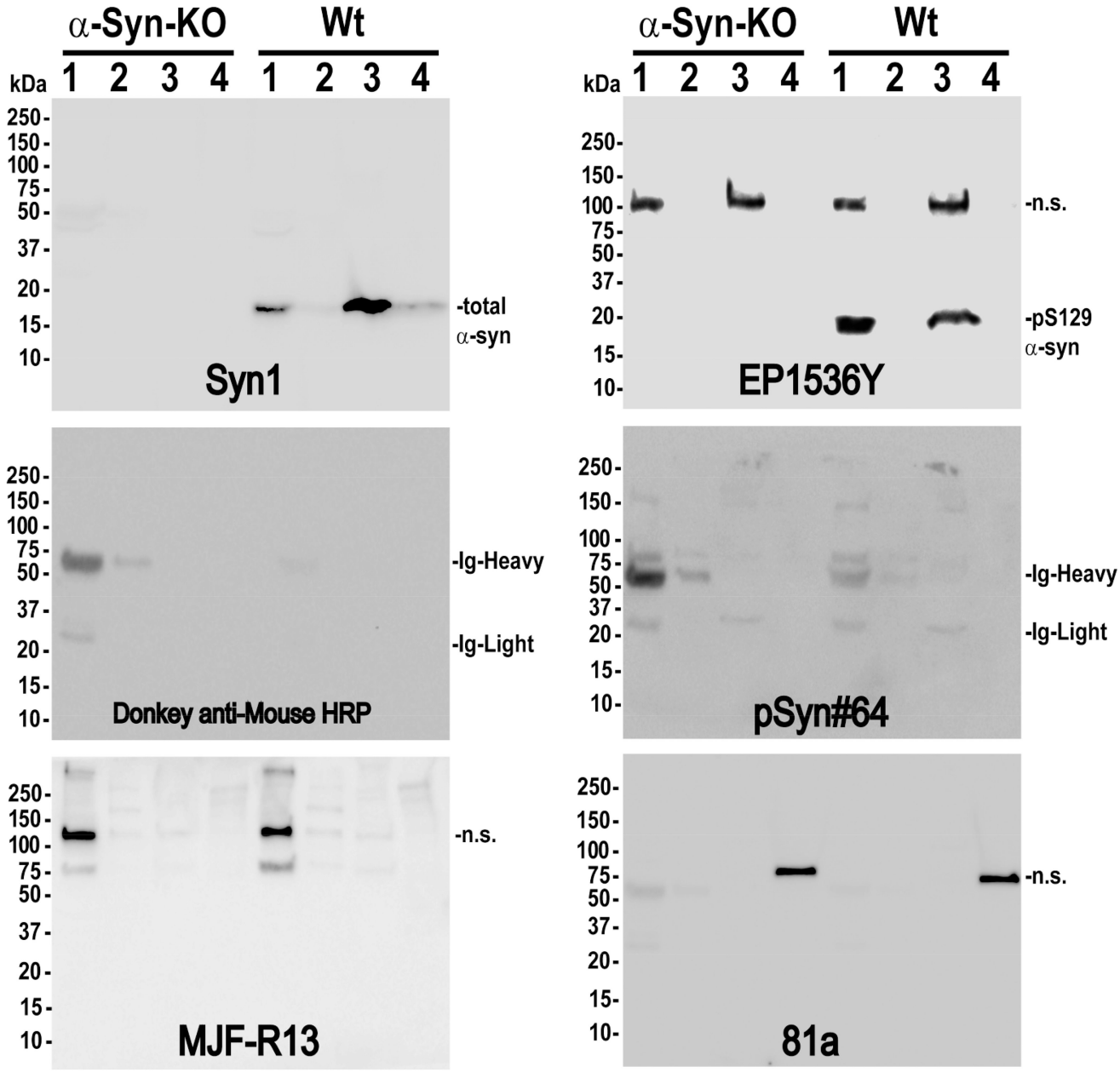

Fig 7. pS129 α-syn monoclonal antibodies detect off-target proteins in brain lysates

Cortical tissue was dissected from wild-type and α-syn knockout mice (C57bl/6J), as indicated, and sequentially processed into buffers of increasing stringency, starting with [lane] 1) saline, 2) high-salt supplemented saline, 3) triton-X 100, and 4) SDS. Molecular weight markers are shown in left margins. The Syn1 monoclonal antibody was used to label total α-syn protein as a positive control, with a secondary-only membrane incubated with donkey anti-mouse antibody as a negative control to reveal globulins.

Table 1

Antibodies used in this study.

pSYN antibodies	antigen	species, types	catalog info
EP1536Y	alpha-synuclein aa 124–134 (phospho 129)	Rabbit monoclonal	Abcam: ab51253
81a	alpha-synuclein aa 124–134 (phospho 129)	Mouse IgG2a monoclonal	Abcam: ab184674
MJF-R13	alpha-synuclein aa 124–134 (phospho 129)	Rabbit IgG monoclonal	Abcam: ab168381
pSyn#64	alpha-synuclein aa 124–134 (phospho 129)	Mouse IgG monoclonal	Wako USA: 015-25191
Syn1	Rat alpha-synuclein aa 15–123	Mouse IgG1	BD Bioscience: 610786

secondary antibodies	species, types	catalog info
	Horse anti mouse biotinylated	Vector Labs: BA-2001
	Goat anti rabbit biotinylated	Vector Labs: BA-1000
	Goat anti mouse IgG2a alexa-488	Thermo Fisher: A-21131
	Goat anti mouse IgG1 alexa-555	Thermo Fisher: A21127
	Goat anti rabbbit IgG alexa-488	Thermo Fisher: A11034
	Donkey anti mouse HRP	Jackson:715-035-151
	Goat anti rabbit HRP	Jackson: 111-035-045